THE ASTROPHYSICAL JOURNAL, 279:93–111, 1984 April 1

THE RADIO MORPHOLOGY OF BLAZARS AND RELATIONSHIPS TO OPTICAL POLARIZATION AND TO NORMAL RADIO GALAXIES

J. F. C. WARDLE
Physics Department, Brandeis University

RICHARD L. MOORE
Owens Valley Radio Observatory; California Institute of Technology

AND

J. R. P. ANGEL
Steward Observatory, University of Arizona
Received 1983 May 31; accepted 1983 September 19

ABSTRACT

VLA observations of BL Lac objects and highly polarized quasars ("blazars") at 1465 MHz were undertaken to determine the radio structure and to explore relationships with the optical polarization. Maps were made of 16 sources, many of which show structure on the scale of a few arc seconds in addition to unresolved core and more diffuse halo components. The luminosity of the extended structure, presumed to be radiating isotropically, is in line with Fanaroff-Riley (FR) type I radio galaxies but is generally weaker than that of the type II, classical double radio galaxies. An interesting parameter is the ratio of the luminosities of the unresolved and the extended components. This has a wide distribution about a median value of 10 in our sample, compared with median values of 0.08 in FR type I sources and 0.015 in FR type II sources. It is correlated with the optical polarization of the blazars in the sense that the strongly core-dominated sources show widely fluctuating position angles of optical polarization, while those with relatively weak cores show a definite preferred position angle. In these latter sources the radio structure is frequently aligned with the optical polarization.

We interpret these results in terms of relativistic jets, where blazar characteristics are due to relativistically enhanced emission beamed in our direction. Then the misdirected objects of the same type could be FR type I sources, which, like BL Lac objects, are centered on bright elliptical galaxies. Lorentz factors of $\gtrsim 2$ are required to give the needed boost in the luminosity of the compact radio source. This precludes identifying BL Lac objects as a specially oriented subclass of FR type II (classical double) sources, since their space densities are comparable. The observed correlations between the intensity of the radio core and the degree of variability of the optical position angle, and between the orientation of the extended radio structure and the average optical position angle, also follow naturally from this picture.

Subject headings: BL Lacertae objects — interferometry — polarization — quasars

I. INTRODUCTION

In recent years, there has been considerable discussion of relativistic jets playing a central role in active galactic nuclei (AGNs) (Blandford and Rees 1978; Scheuer and Readhead 1979; Blandford and Königl 1979; Marscher 1980). The idea of relativistic bulk motion near the line of sight is motivated largely by observations of "superluminal" motion (e.g., Cohen and Unwin 1982) and low-frequency variability (e.g., Condon *et al.* 1979). If these extreme objects contain jets that make a very small angle to the line of sight, then misdirected relativistic jets must also exist in many active galactic nuclei. The orientation effects of relativistic jets may well account for a number of the observed properties of different classes of AGNs.

BL Lac objects and highly polarized quasars are important classes of AGNs because they are thought to be examples of relativistic jets seen nearly end-on. Generally, these objects are compact, core-dominated radio sources, exhibit rapid radio and optical variability, have high, variable optical polarization, and often exhibit low-frequency variability and/or "superluminal" expansion (Angel and Stockman 1980; Moore and Stockman 1981). The rapid variability and extreme properties are attributed to relativistic motion of the emitting material and the consequent Doppler enhancement of the core component by large factors relative to any quasi-stationary emitting region.

There are several predictions of the relativistic jet model concerning BL Lac objects and highly polarized quasars which can be tested. First, while most highly polarized objects are core-dominated radio sources, it is clear that many contain some extended radio structure. A few individual cases have been known for some time (e.g., Conway and Stannard 1972; Gopal-Krishna 1977; Margon, Jones, and Wardle 1978). Based on an extensive monitoring program with an interferometer, Wardle (1978) reported that 13 of 26 BL Lac objects showed some sort of extended structure. Weiler and Johnston (1980) surveyed all known BL Lac objects and found that 22 out of 40 contained extended structure. VLA surveys by Perley (1982) and Ulvestad *et al.* (1981) showed this to be a fairly common property of flat-spectrum radio sources in general.

One possible interpretation of this extended structure follows naturally from the Scheuer and Readhead (1979) picture of compact radio sources. That is, we are looking at "normal" double radio sources, such as comprise the great majority of 3CR sources, nearly end-on (along their major axis), and the relative intensity of the central component is greatly enhanced by the Doppler effect.

This interpretation can be tested by making high dynamic range maps of BL Lac objects to determine the structure and intensity of the extended radio structure. If BL Lac objects are doubles seen end-on, the luminosity of the unenhanced emission should be comparable to that of normal 3CR double sources. Second, the relative intensity of the core to the extended emission should reflect the Lorentz factor of the jets and the distribution of angles to the line of sight. It is possible to test the model by examining the distribution of the ratio of core to extended emission.

Another aspect of the relativistic jet model we wish to explore is whether there is a relationship between the radio structure of BL Lac objects and their optical polarization. Rapid polarimetric variability is characteristic of nearly all BL Lac objects (Angel and Stockman 1980). However, an important phenomenom discovered by Angel *et al.* (1978) is that about half of BL Lac objects exhibit a "preferred" position angle of optical polarization; the angle is variable but restricted within a range of 15° over time scales of years (much longer than the characteristic time scale of the variations). This phenomenon has been confirmed for a much larger sample of BL Lac objects based on all available polarimetric observations (Moore 1983).

If the optical emission is produced in a jet, symmetry arguments imply that, for small angles to the line of sight, the position angle of polarization is less likely to be preferred. This is particularly true if the optical-emitting material is moving relativistically, in which case small changes in the jet direction, magnetic field, or Lorentz factor may lead to wild fluctuations in the position angle of polarization (Blandford and Königl 1979). Thus, we could expect that the jets in preferred-angle objects are more likely to make a larger angle to the line of sight. Correspondingly, these objects may be more likely to exhibit relatively stronger extended radio emission.

Finally, for objects with a preferred angle of optical polarization, it is important to determine whether this angle is correlated with the orientation of extended radio structure. A systematic alignment of these angles has been found among low-polarization quasars (Stockman, Angel, and Miley 1979; Moore and Stockman 1981) and among radio galaxies (Antonucci 1982). Although the origin of the polarization in highly polarized objects is likely to be different from that of the low-polarization AGNs, a similar relationship would imply that the compact, optical-emitting region of BL Lac objects also has a long-term memory. If the optical emission of BL Lac objects is indeed synchrotron radiation (Angel and Stockman 1980), a correlation of position angles would tie the magnetic field structure of the central region to the collimation mechanism for the radio emission.

It is crucial for addressing these questions concerning BL Lac objects to obtain high dynamic range radio maps of the small-scale extended structure. Therefore, we have used the VLA to make maps of 16 BL Lac objects and highly polarized quasars. The objectives of these observations are to determine the radio morphology, explore the relationship between radio structure and optical polarization, and test the predictions of the relativistic jet model. The objects were chosen from the list of Angel and Stockman (1980) to include a number of preferred-angle sources and sources with a substantial low-frequency component. A wavelength of 20.5 cm was chosen to enhance the contrast of the steep-spectrum extended emission relative to the core components.

In § II, we describe the observations and mapping techniques. The observational results are tabulated and discussed in § III; comments on individual sources follow in § IV. The relationship between radio structure and optical polarization is discussed in § V. We address in § VI whether the radio structure of BL Lac objects is consistent with the relativistic jet model. The results are summarized in § VII.

II. OBSERVATIONS

The observations were made on 1980 June 12–13 using 19 antennas of the partially completed Very Large Array (Thompson *et al.* 1980), operating at a frequency of 1465 MHz (20.5 cm), with a bandwidth of 50 MHz. The antennas were arranged in a hybrid configuration with separations ranging from 50 m to 24 km.

Each source was observed for a total integration time of about 1 hr, divided into scans of 5 minutes duration spread over the available range of hour angles. A calibration source was observed once every hour to monitor gain and phase changes in the array. The calibrators and their assumed flux densities are listed in Table 1. The flux density scale was set to that of Baars *et al.* (1977) by brief observations of 3C 286. The instrumental polarization of the array was checked by assuming that 0316+161, 1404+286, and 2134+004 are unpolarized. Recent measurements by Perley (1982) show that the degrees of linear polarization of these three sources at this wavelength are 0.3%, 0.4%, and 0.2%, respectively. The polarization scale and position angle zero were also set by the observations of 3C 286.

Preliminary editing and calibration were performed at the VLA site. The final calibration and map-making was carried out at NRAO[1] in Charlottesville. The data were

[1] NRAO is operated by Associated Universities, Inc., under contract with the National Science Foundation.

TABLE 1

CALIBRATION SOURCES

Source	Flux Density (Jy)	Linear Polarization m (%)	Linear Polarization χ (degrees)
0316+162	7.73	<1	...
0727−115	1.77	...	...
0742+103	3.47	...	...
3C 287	6.77	...	...
3C 286	14.41	9.98	33
1404+286	0.83	<1	...
2134+004	3.58	<1	...

gridded in the *u-v* plane, and a convolution was applied to reduce the effects of aliasing. Maps were made with the FFT and then CLEANed in the usual way (Hogböm 1974).

The initial maps were of poor quality, with a signal-to-noise ratio of only about 20:1. This was due to bad weather during the observing run, which resulted in large atmospheric phase fluctuations. Since all the sources observed contain compact components which are unresolved on the longest baselines, we applied the "self-calibration" technique described by Perley, Fomalont, and Johnston (1980). This resulted in a dramatic improvement in the quality of the maps, most of them achieving a signal-to-noise ratio of better than 200:1. This high dynamic range is essential to search for low-brightness extended structure surrounding the compact components.

The accuracy of the final maps is still limited by dynamic range rather than system noise. This is due to antenna gain fluctuations (to which we did not apply the self-calibration technique) and to errors in the self-calibration procedure when there is extended structure present that is not entirely resolved on the longest baselines. This latter effect is most severe for the three well-resolved sources 0521−365, 0752+258, and 1400+162.

A further problem with this self-calibration scheme is that small positional uncertainties may be introduced. By comparing maps made before and after the self-calibration, we believe these errors are not larger than 0″.5. Also, we did not observe phase calibrators often enough to obtain absolute positions of astrometric quality. We have compared our final positions for the compact radio components with the positions given by Perley (1982), which are of high accuracy, and find that the rms error in our absolute positions is 0″.7. The single exception is the source 0521−365, where the combination of bad atmospheric conditions and very low declination has led to an error of 4″ in the final map (see below).

III. RESULTS

We have divided the sources into two groups: 13 whose structure is dominated by an unresolved component, and three dominated by extended structure. The parameters of the sources in the first group are listed in Table 2, and maps of 11 of them are shown in Figures 1*a*–1*i*. The parameters and maps of the extended sources are given in Table 3 and Figures 2*a*–2*d*, respectively. Details concerning the maps are given in the legends to Figures 1 and 2.

The meaning of the columns in Table 2 is as follows: Column (1) lists the name of the source in the usual Parkes notation. Column (2) gives the total flux density at 1465 MHz. This is taken directly from the fringe amplitude measured on the shortest baselines. At this frequency the rms confusion is about 100 mJy on short baselines. It is difficult to distinguish between confusion and a possible very large "halo" component, so generous errors have been assigned.

The way in which we have described the morphology of the radio structures, in column (3), requires explanation. The maps in Figure 1 reveal a variety of morphologies. Two sources (0422+004, 2254+074) consist of a single unresolved (<0″.5) component coincident with the optical nucleus. These are denoted by C in column (3). The sources 0829+046, 1133+704, and 1727+502 also have simple structures, consisting of an unresolved component coincident with the optical nucleus together with a large halo of extended emission surrounding the compact source. These are denoted by CH in column (3). We do not show maps of the above five sources.

The other eight sources in Table 2 also contain an unresolved component coincident with the optical nucleus, often with a halo of extended emission, but also with significant structure on a scale of a few arc seconds. The presence of large-scale structure is again denoted by H. The small-scale structure is more difficult to characterize. In two sources (0048−097, 2345−167) this consists of a single component to one side of the unresolved source. This morphology is denoted by D2, following Miley (1971).

The remaining six sources exhibit the most interesting morphology. In each case the small-scale structure is definitely elongated on both sides of the nuclear component. It might be possible to interpret these structures as "two-sided jets," but we consider this premature. First, the "self-calibration" procedure may have introduced small uncertainties in the relative position and intensity of features in the maps. Second, in the maps of these sources shown in Figure 1, a point source has been subtracted at the position of the nuclear component. The appearance of the resulting contour map depends critically on the value assumed for the flux density of this component. Subtracting too little leaves a single elongated residual component. Subtracting too much leaves a distinct double structure. If the small-scale structure is both faint and only a few beamwidths in extent, then there is an inevitable uncertainty in determining its true nature. In view of these uncertainties we describe the small-scale structure as barlike and denote it by a B in column (3).

Columns (4)–(6) list the flux density and position of the unresolved nuclear component. The value for the flux density is not necessarily the value subtracted from the maps in Figure 1. The former is the fringe amplitude observed on the longest baselines. The latter is simply the flux density of the strongest point component found by the CLEAN algorithm operating on the original "dirty" map prior to the "self-calibration" procedure.

Columns (7)–(10) list the flux density, position relative to the compact component, angular extent, and orientation of the small-scale structure. In view of the uncertainties discussed above, we do not list positions for the "bar" structures. Approximate positions may be inferred from the maps.

Columns (11)–(13) list the flux density, angular extent, and orientation of the large-scale "halo" components.

Table 3 lists the parameters for the three sources dominated by extended structure, whose maps are shown in Figure 2. Column (1) gives the name of the source and then the features for which we list parameters. Columns (2) and (3) give the position of the optical nucleus and then the positions of other features relative to the optical positions, in arc seconds. The optical positions are taken from R. A. E. Fosbury (personal communication) for 0521−365, Wills and Wills (1976) for 0752+258, and Murdoch (1976) for 1400+162.

Columns (4)–(6) list the flux densities, angular sizes, and orientations of the radio structures. The "total radio" flux density is taken from the fringe amplitude measured on the

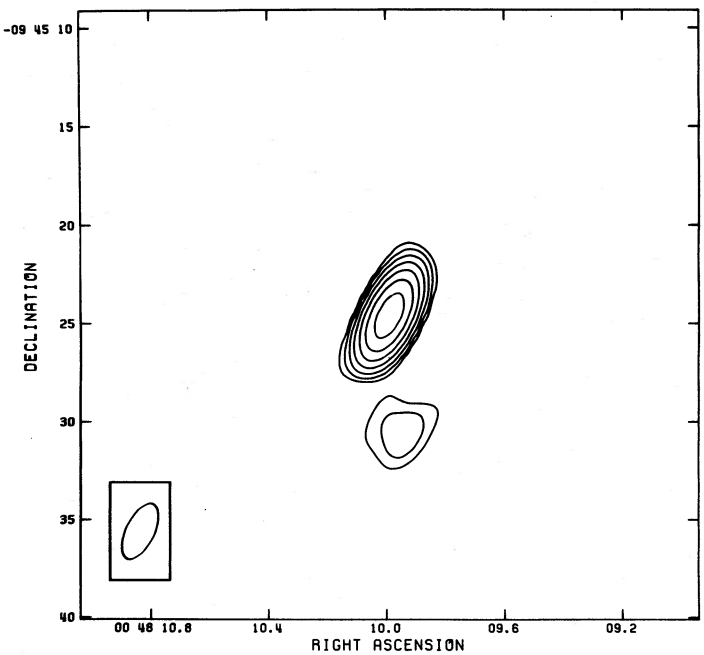

FIG. 1*a*

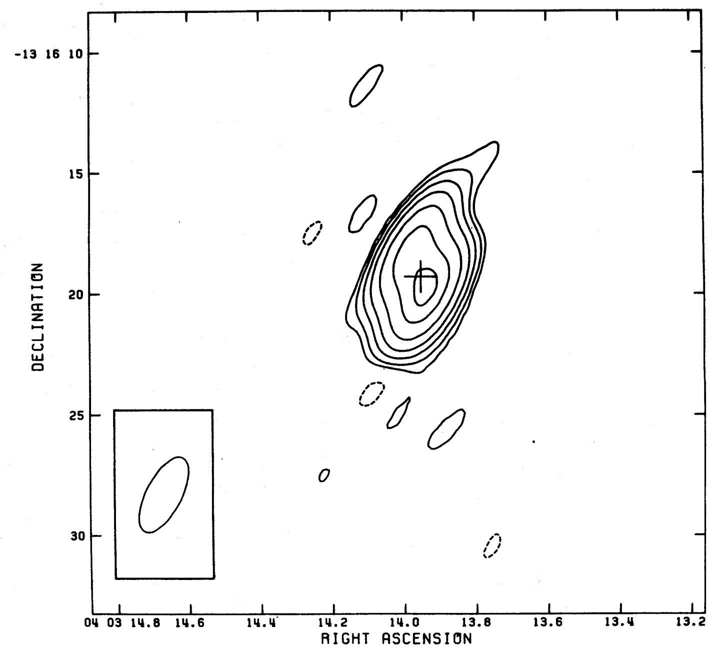

FIG. 1*b*

FIG. 1.—Maps of the sources listed in Table 2. Unless stated otherwise, no taper has been applied in the *u-v* plane. The restoring beam is given by the boxed ellipse in the corner. Negative contours are shown broken. When a point source has been subtracted from the data, its position is marked with a cross. (*a*) 0048−097: Contour levels = (1, 2, 4, 8, 16, 32, 64)% × 870 mJy. (*b*) 0403−132: 3009 mJy point source removed. Contour levels = (2, 4, 8, 15, 30, 60, 90)% × 626 mJy. (*c*) 0818−128: 529 mJy point source removed. Contour levels = (2, 4, 8, 15, 30, 60, 90)% × 124 mJy. (*d*) 3C 216 = 0906+430: 1896 mJy point source removed. Contour levels = (2, 4, 8, 15, 30, 60, 90)% × 688 mJy. (*e*) 1215+303: 333 mJy point source removed. Contour levels = (10, 20, 30, 50, 70, 90)% × 17 mJy. (*f*) 2155−152: 1160 mJy point source removed. Contour levels = (3, 6, 12, 24, 40, 60, 90)% × 90 mJy. (*g*) 2155−304: 227 mJy point source removed. Contour levels = (10, 20, 40, 60, 90)% × 14 mJy. (*h*) 2155−304: Gaussian taper applied to the *u-v* plane, width 3000λ to half-power. 227 mJy point source removed. Contour levels = (5, 10, 15, 20, 25, 50)% × 26 mJy. (i) 2345 − 167: Contour levels = (0.5, 1.0, 1.5, 2.0, 2.5, 5, 10, 50)% × 2487 mJy.

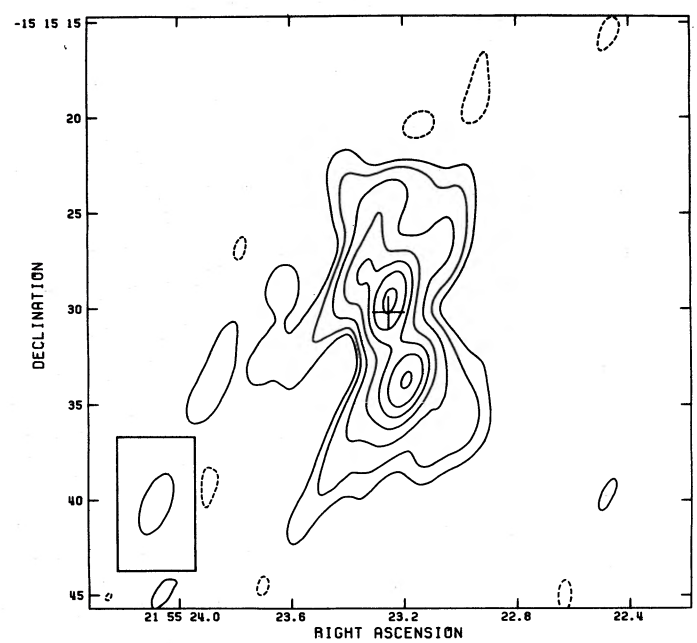

FIG. 1*f*

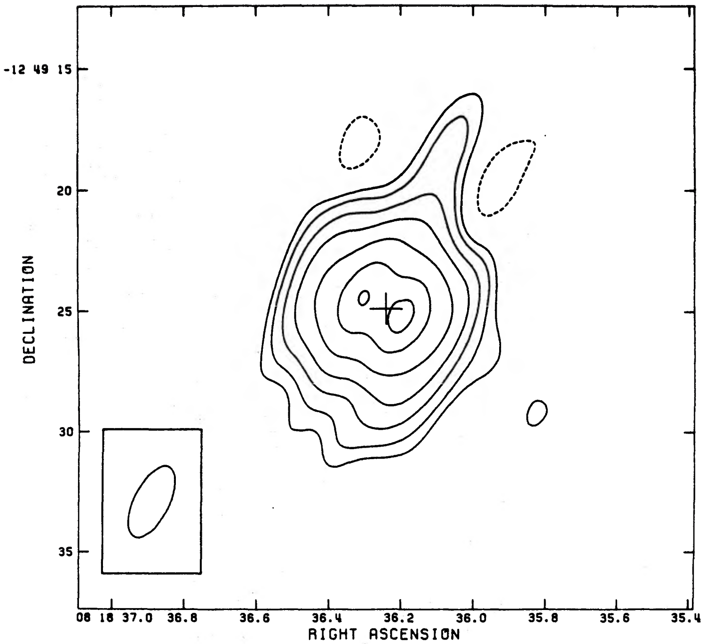

FIG. 1c

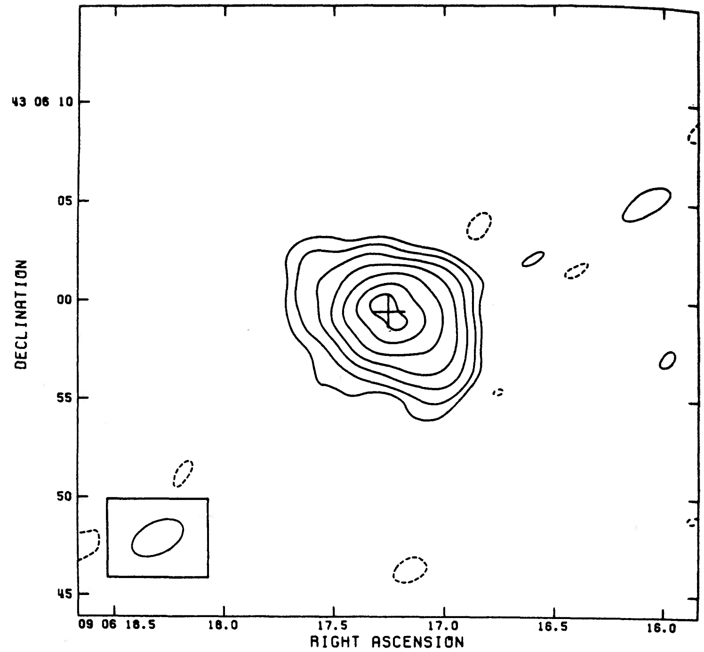

FIG. 1d

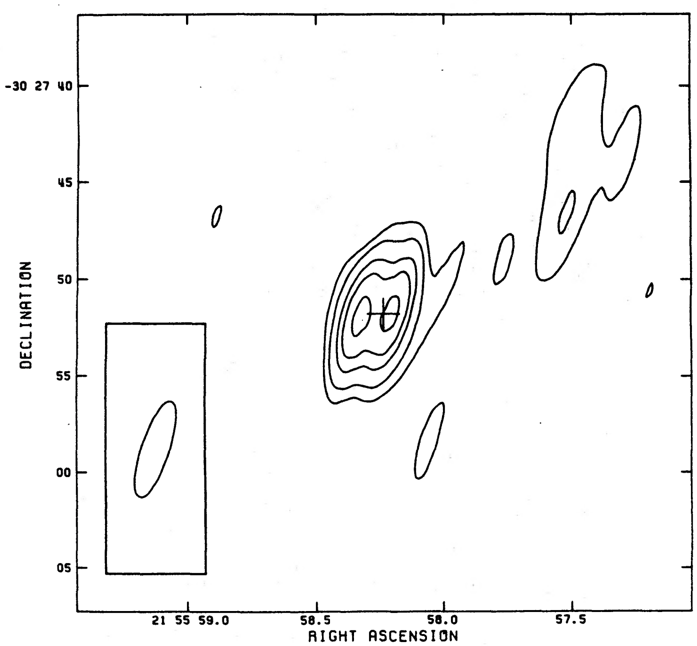

FIG. 1g

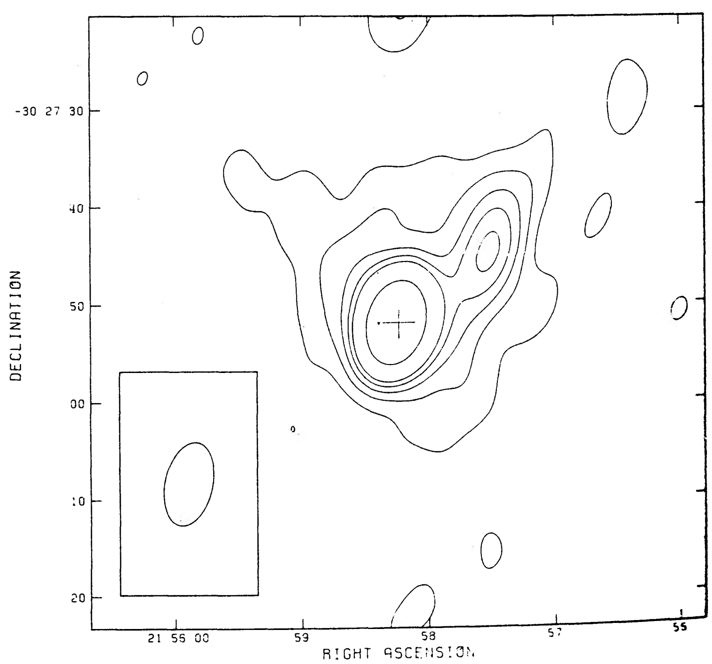

FIG. 1h

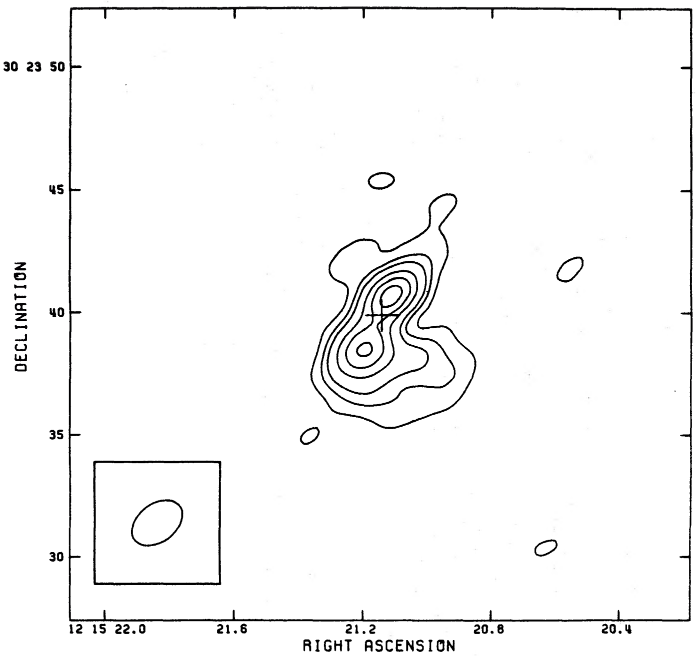
30 23 50
45
40
35
30
DECLINATION
12 15 22.0
21.6
21.2
20.8
20.4
RIGHT ASCENSION

FIG. 1*e*

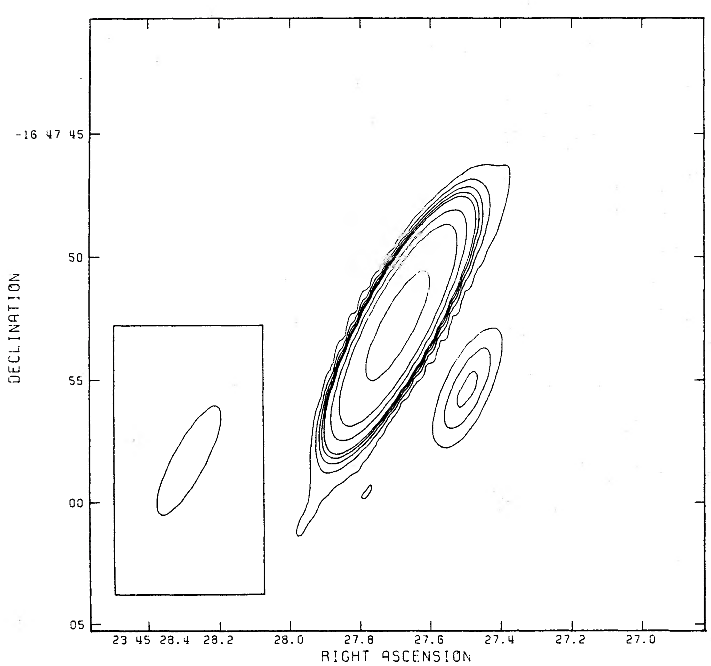
-16 47 45
50
55
00
05
DECLINATION
23 45 28.4
28.2
28.0
27.8
27.6
27.4
27.2
27.0
RIGHT ASCENSION

FIG. 1*i*

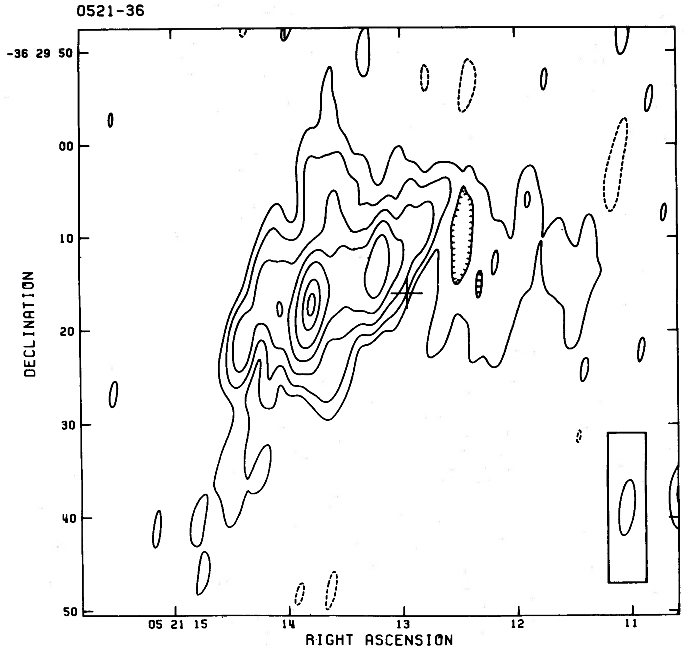

FIG. 2*a*

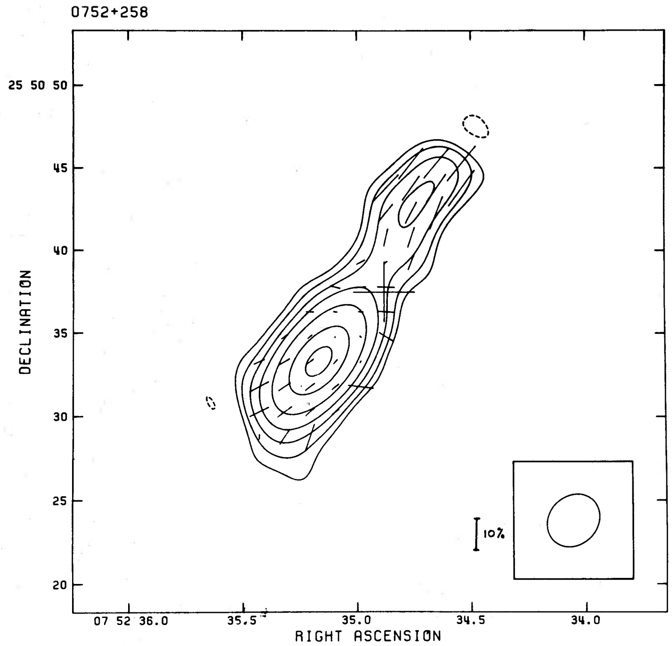

FIG. 2*b*

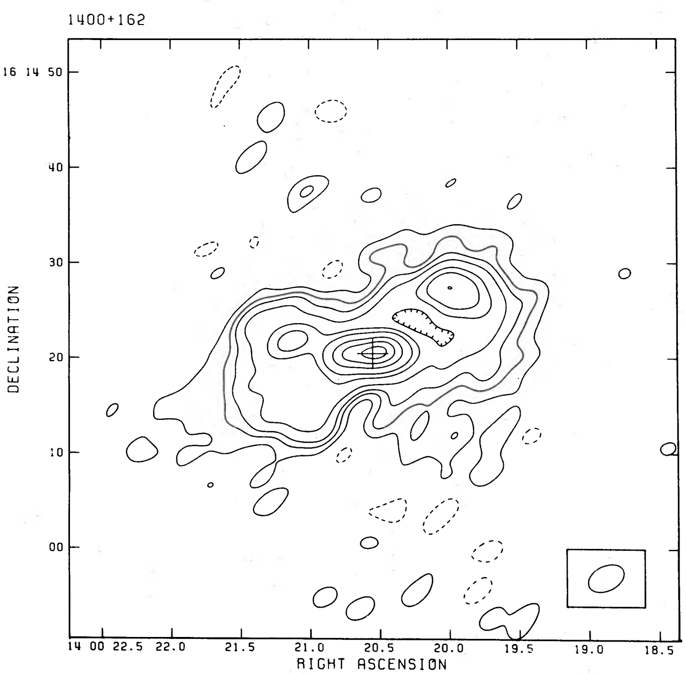

FIG. 2*c*

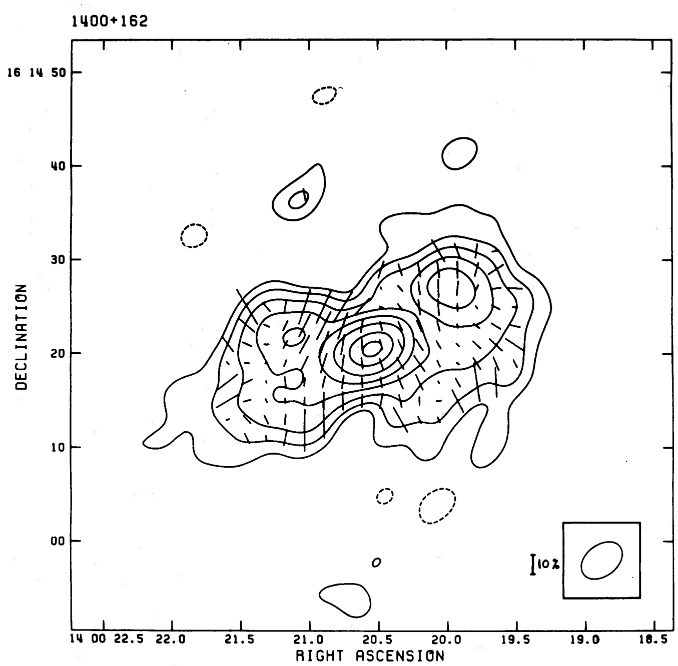

FIG. 2*d*

FIG. 2.—Maps of the sources listed in Table 3. Negative contours are shown as broken lines. The restoring beam is given by the boxed ellipse in the corner. The length of the polarization vectors gives the percentage linear polarization, and their orientation is that of the electric vectors. The scale of the polarization is given by the bar near the resolution ellipse. (*a*) 0521 − 365: No taper applied to the *u-v* plane. Contour levels = (1.5, 3, 6, 12, 25, 60, 90)% × 3087 mJy. The cross marks the optical position found by R. A. E. Fosbury (personal communication); see comments in § IV. (*b*) 0752 + 258: Gaussian taper applied to the *u-v* plane, width 60000λ to half-power. Contour levels = (2, 4, 8, 15, 30, 60, 90)% × 172 mJy. The cross marks the optical position given by Wills and Wills (1976). (*c*) 1400 + 162: No taper applied to the *u-v* plane. 164 mJy point source has been subtracted at the position of the cross (see Table 3). Contour levels = (2, 4, 6, 10, 20, 30, 50, 70, 90)% × 96 mJy. (*d*) 1400 + 162: Gaussian taper applied to the *u-v* plane, width 50000λ to half-power. No point source has been removed. Contour levels = (1, 2, 4, 8, 15, 30, 60, 90)% × 276 mJy.

TABLE 2

SOURCES DOMINATED BY AN UNRESOLVED COMPONENT

Source (1)	Total Flux Density (Jy) (2)	Morphology (3)	Point Source: Flux Density (Jy) (4)	Point Source: R.A. (1950.0) (5)	Point Source: Decl. (1950.0) (6)	Small-Scale Structure: Flux Density (Jy) (7)	Small-Scale Structure: Relative Position (arcsec) (8)	Small-Scale Structure: Angular Size (arcsec) (9)	Small-Scale Structure: Position Angle (degrees) (10)	Large-Scale Structure: Flux Density (Jy) (11)	Large-Scale Structure: Angular Size (arcsec) (12)	Large-Scale Structure: Position Angle (degrees) (13)
0048−097	0.96 ± 0.10	D2	0.87 ± 0.02	$00^h48^m10^s.00$	−09°45′24″.6	0.05 ± 0.01	0.7 W 6.0 S	~2	...	...	...	...
0403−132	4.20 ± 0.30	CB	3.00 ± 0.20	04 03 13.93	−13 16 19.3	1.16 ± 0.05	...	2 × <2	23	...	...	...
0422+004	1.42 ± 0.15	C	1.35 ± 0.07	04 22 12.57	00 29 17.6	<0.05	...	...	...	...	...	...
0818−128	1.03 ± 0.06	CBH	0.48 ± 0.02	08 18 36.23	−12 49 24.4	0.31 ± 0.02	...	5 × <2	73	0.25 ± 0.03	~8	...
0829+046	0.80 ± 0.05	CH	0.62 ± 0.02	08 29 10.90	04 39 51.1	<0.04	...	...	...	0.18 ± 0.02	~30	...
0906+430	4.10 ± 0.25	CBH	1.30 ± 0.20	09 06 17.35	43 05 58.9	1.66 ± 0.10	...	2 × <2	45	1.03 ± 0.10	12 × 8	60
1133+704	0.36 ± 0.04	CH	0.13 ± 0.01	11 33 32.39	70 26 03.0	...	...	...	...	0.23 ± 0.02	≥50	...
1215+303	0.56 ± 0.04	CBH	0.34 ± 0.03	12 15 21.14	30 23 39.9	0.03 ± 0.01	...	3 × <1	154	0.18 ± 0.02	40 × 20	45
1727+502	0.22 ± 0.02	CH	0.17 ± 0.01	17 27 04.35	50 15 30.7	<0.01	...	...	...	0.05 ± 0.02	>10	...
2155−152	1.57 ± 0.11	CBH	1.20 ± 0.07	21 55 23.17	−15 15 30.2	0.14 ± 0.02	...	4 × ≤2	14	0.23 ± 0.03	15 × 7	0
2155−304	0.34 ± 0.04	CBH	0.22 ± 0.02	21 55 58.32	−30 27 54.8	0.03 ± 0.01	...	2 × <2	90	0.09 ± 0.01	~25	...
2254+074	0.46 ± 0.04	C	0.43 ± 0.02	22 54 45.97	07 27 08.7	<0.02	...	...	...	...	...	...
2345−167	2.69 ± 0.15	D2	2.49 ± 0.08	23 45 27.70	−16 47 52.8	0.06 ± 0.01	3.0 W 2.5 S	~2	...	...	...	...

TABLE 3

SOURCES DOMINATED BY EXTENDED STRUCTURE

SOURCE/COMPONENT (1)	R.A. (1950.0) (2)	Decl. (1950.0) (3)	FLUX DENSITY (Jy) (4)	ANGULAR SIZE (arcsec) (5)	POSITION ANGLE (degrees) (6)	LINEAR POLARIZATION m (%) (7)	LINEAR POLARIZATION χ (degrees) (8)
0521−365:							
Optical	$05^h21^m12^s.93$	−36°30′16″.0	...	...	...	...	...
Total radio	...	...	15.5 ± 1.5	40 × 25	110	<2	...
Np	2″.7 E	3″.1 N	1.4 ± 0.1	≤2	...	...	...
Sf	9″.8 E	1″.3 S	2.6 ± 0.2	≤2	...	...	...
0752+258:							
Optical	$07^h52^m34^s.88$	25°50′37″.5	...	...	...	...	...
Total radio	...	...	0.40 ± 0.10	19 × 2	145	2.3 ± 1.0	~135
Np	1″.6 W	5″.3 N	0.06 ± 0.01	8 × 2	147	4.7 ± 0.8	~144
Sf	3″.9 E	4″.2 S	0.30 ± 0.02	11 × 2	144	1.9 ± 0.5	~130
1400+162:							
Optical	$14^h00^m20^s.52$	16°14′20″.9	...	...	...	...	...
Total radio	...	...	0.80 ± 0.08	35 × 15	~120	4.4 ± 1.0	~5
Central	0″.1 E	0″.4 S	0.16 ± 0.01	<2	...	0.9 ± 0.5	~0
"Jet"	1″.8 E	0″.4 S	0.12 ± 0.02	3.5 × <2	90	16.4 ± 2.0	~10

shortest baselines. All other parameters are taken directly from the maps.

Columns (7) and (8) give the percent linear polarization and the orientation of the electric vector. These were determined by summing appropriate areas on the CLEANed maps of the Stokes parameters Q and U (made after the instrumental polarization of the array was removed in the usual way). No correction has been made for Faraday rotation in the ionosphere. At 1465 MHz this typically ranges between 5° at night and as much as 40° at noon (depending also on the azimuth and elevation of the observations, and on the level of solar activity). The position angles given in column (8) are therefore only approximate.

IV. NOTES ON THE INDIVIDUAL RADIO SOURCES

a) 0048−097 = OB−080

This is a lineless BL Lac object. It is an optically violent variable (OVV) (Usher, Kolpanen, and Pollock 1974) and exhibits strong and variable optical polarization (Kinman 1976). It is also well-known variable radio source with a flat spectrum (e.g., Altschuler and Wardle 1976; Kesteven, Bridle, and Brandie 1976; Andrew *et al.* 1978). The single secondary component that we observed is also found by Perley (1982), using the VLA at 20 cm. At 6 cm he finds no extended structure brighter than 0.4% of the compact core. This is consistent with the angular size we have assigned to the secondary component. However, Weiler and Johnston (1980) find evidence for extended structure containing 0.1 Jy at 6 cm, from limited VLA observations, and Wardle, Bridle, and Kesteven (1981) find extended structure containing 0.13 ± 0.02 Jy at 11.1 cm, from a combination of interferometer and single-dish observations. It is therefore possible that the present observations have missed a faint halo associated with this source, or there may be a flat-spectrum, confusing source in the field.

b) 0403−132

This is a quasar with a redshift of 0.571 (Hewitt and Burbidge 1980). Optically, it is moderately variable and modestly polarized (Moore and Stockman 1981). In the spectral compilation by Kühr *et al.* (1981), this source is probably variable at 6 cm. The shape of the spectrum is complex, and they quote a spectral index between 6 and 11 cm of $\alpha = -0.14$ ($S \propto \nu^{\alpha}$). The average of three flux densities at 20 cm is 4.22 ± 0.05, in agreement with our value. Our value for the flux density of the compact component is rather uncertain because the extended structure is not fully resolved on the longest spacings. However, this structure is definitely extended on both sides of the compact component, and we have denoted it as barlike in Table 2.

c) 0422+004 = OF 038

This a lineless BL Lac object which is an OVV (Pica *et al.* 1980). It exhibits strong and variable optical polarization with a preferred position angle (Angel *et al.* 1978). It is a strongly variable radio source at all wavelengths (Fanti *et al.* 1979, 75 cm; Kesteven, Bridle, and Brandie 1976, 11.1 cm; Altschuler 1982, 12.6 cm; Landau, Epstein, and Rather 1980, 3.3 mm). Weiler and Johnson (1980) find no evidence for extended structure at 6 or 2 cm. Perley (1982) sets an upper limit on the peak brightness of any secondary structure at 20 cm of 1.5% of the compact component. His corresponding limit at 6 cm is 0.3%. He measured a total flux density at 20 cm of 0.98 Jy on 1981 February 18–19. The source has therefore dimmed by 45% in the 8 months following our observations. He also notes the presence of confusion at 20 cm. We have made a large field-of-view map to try and locate the confusing source. We conclude that it is more distant than 10′ from the BL Lac object and has a flux density ≥0.6 Jy.

d) 0521−365

This is a giant elliptical galaxy with weak emission lines ($z = 0.061$); it is associated with a luminous extended steep-spectrum radio source (Danziger *et al.* 1979). The nucleus is optically variable (Usher 1975). We have made two measurements of the optical polarization, in 1979 October and 1980 January. Both measurements are consistent with $P = 5.6\% \pm 0.3\%$ and $\theta = 153° \pm 2°$. From brief observations with the VLA at 6 cm, Danziger *et al.* found a compact 1 Jy radio component coincident with the optical nucleus. A more recent VLA map made by R. D. Ekers (personal communication) confirms this positional coincidence. It is clear that our map (Fig. 2*a*) contains a positional error of about 4″. The "north preceding" component listed in Table 3 should be coincident with the optical nucleus. If the whole map is shifted in this way, then it is in good agreement with Ekers's map. The gross structure of the radio source is diffuse and elongated rather than double and is very much larger than the elliptical galaxy. The spectral indices between 6 and 20 cm of the compact components are $\alpha \sim -0.3$ (nucleus) and $\alpha \sim -1.0$ (Sf). The overall spectral index for the source is $\alpha = -0.45$ (Kühr *et al.* 1981). The line from the nucleus to the Sf component has a position angle of $109° \pm 15°$. This is nearly parallel to, but oppositely directed from, the optical jet described by Danziger *et al.*, which has a position angle of 305°.

e) 0752+258 = OI 287

This source was identified by Wills and Wills (1976), who found strong sharp forbidden lines of [O II] and [O III] but no Balmer lines. They comment that on spectroscopic evidence alone, it could be classified as a galaxy, though the appearance is stellar. The redshift is 0.446. Moore and Stockman (1981) found strong and essentially constant optical polarization of 8% at position angle 144°. The radio map (Fig. 2*b*) has the appearance of a normal double source, but maps made from untapered data show the width of the radio source transverse to its major axis is less than 2″ along its entire length, perhaps more reminiscent of twin "jets." However, there are no clear hot spots at the ends of these features (there is some evidence that the Sf component may flare out into a very diffuse lobe of faint radio emission), and there is no compact radio component near the optical position with a flux density greater than 10 mJy. The radio source exhibits a moderate degree of linear polarization, with the electric vectors predominantly parallel to the source axis and to the optical polarization. Such an alignment would be similar to that found in large-scale galactic radio jets (Bridle 1982), but this may be entirely fortuitous. We have not corrected for ionospheric Faraday rotation, and the Galactic contribution is quite uncertain. The Galactic coordinates are $l = 196°$, $b = 25°$, and nearby radio sources exhibit rotation measures ranging from -1 to $+89$ radians m^{-2} (Simard-Normandin, Kronberg, and Button 1981). Clearly higher frequency, higher resolution observations of this source would be of the greatest interest.

f) 0818−128 = OJ−131

This is a lineless BL Lac object. At 6 cm, Weiler and Johnston (1980) find it to contain 0.23 Jy in extended structure which is about 4″ in size. This is consistent with our observations and shows the extended structure to have a normal spectrum ($\alpha \sim -0.7$). They find a spectral index for the compact component of $+0.12$ between 6 and 2 cm. We do not know if the source is a radio variable, though it is certainly variable at optical wavelengths and exhibits strong and variable optical polarization with a preferred position angle (Angel and Stockman 1980).

g) 0829+046 = OJ 049

This is a lineless BL Lac object. Weiler and Johnston find it to consist of a compact core and a halo 30″ in extent that contains 0.06 Jy at 6 cm. This is in agreement with our results, and the halo has a steep spectrum ($\alpha \sim -0.9$). Kesteven, Bridle, and Brandie (1976) did not observe the source to vary at 11.1 cm. It is certainly variable at 3.7 cm (Wardle 1978) and at optical wavelengths (Usher 1975), where it is also strongly polarized (Angel and Stockman 1980).

h) 0906+430 = 3C 216 = 4C 43.17 = OK 410

This is a quasar with strong emission lines and a redshift of $z = 0.67$ (Hewitt and Burbidge 1980). The optical polarization is strong and variable (Kinman 1976; Moore and Stockman 1981), but it is not known to what extent the continuum magnitude varies. At centimeter wavelengths the source has not been observed to vary (Kesteven, Bridle, and Brandie 1976; Altschuler and Wardle 1976; Andrew *et al.* 1978). Ulvestad *et al.* (1981), from brief observations with a seven antenna subarray of the VLA, find the source to be "slightly extended in position angle 30°." At 6 cm they observe a peak flux density of 1.0 Jy and a total flux density of 1.8 Jy. At 20 cm their corresponding numbers are 3.1 and 4.2 Jy. If their peak flux density of 3.1 Jy is taken to include both the compact source and what we have denoted as small-scale structure in Table 2, then the two sets of observations are in excellent agreement. Although the precise values are not clear, the compact source has a fairly flat spectrum, and the extended structure has a steep spectrum. It is certain that this source contains structure on several angular scales because the mean fringe amplitude starts to fall off even at very short distances in the *u*-*v* plane and declines steadily to longer *u*-*v* distances.

i) 1133+704 = Mrk 180

This is a galaxy with a redshift of 0.044 (Miller, French, and Hawley 1978) and modest optical polarization (Angel and Stockman 1980). Because of bad weather, we ended up with only a single 8 minute "snapshot" of this source. The gross structure is undoubtedly "core-halo," but the data are of insufficient quality to set useful limits on possible small-scale structure in the vicinity of the compact component.

j) 1215+303 = ON 325

This is a lineless BL Lac object which is optically variable and exhibits strong and variable optical polarization with a preferred position angle (Angel *et al.* 1978). It is also a radio variable (Wardle 1978). At 6 cm, Weiler and Johnston found 0.1 Jy in an extended component of size 36″. At 20 cm, Ulvestad, Johnston, and Weiler (1983) find 0.15 Jy in an extended component of size $\sim 50''$ elongated in position angle $\sim 75°$. These results are in adequate agreement with the large-scale structure listed in Table 2. At 6 cm, Ulvestad *et al.* find 0.05 Jy in extended structure, so the halo component has a steep spectrum. The spectral index of the compact component is $\alpha = 0.08$. The observations of Ulvestad *et al.* are of comparable quality to our own, but they do not show a high-resolution map of 1215+303, so it is not clear if they see the small-scale structure we have found. If this has a steep spectrum, it might be difficult to see at 6 cm.

k) 1400+162 = 4C 16.39 = OQ 100

This is a galaxy with weak emission lines ($z = 0.244$); its nucleus has an essentially continuous spectrum and exhibits strong and variable optical polarization (Baldwin *et al.* 1977). It is a member of a small group of galaxies, the nearest of which is only 6″ to the southwest and has the same redshift. Baldwin *et al.* also present a map made with the Cambridge 5 km telescope at 6 cm which shows that 62% of the flux comes from extended regions (of total extent $\sim 25''$) on either side of the compact source. This is the first BL Lac object whose radio structure could loosely be classified as double. The compact source has a flat spectrum, and the extended structure has a spectral index $\alpha \sim -0.7$. Good maps made with the VLA at 20 cm have been presented by Hintzen and Owen (1981), and our maps (Figs. 2*c*–2*d*) are in excellent agreement. Hintzen and Owen point out that the radio structure is bent, probably as a result of interaction with intracluster gas, and is reminiscent of the wide-angle radio tail sources found in many clusters of galaxies (Owen and Rudnick 1976). There are no "hotspots" at the outer edges of the radio lobes, but the central component is extended, pointing toward the eastern lobe. At our resolution this is suggestive of a radio "jet." Higher resolution observations by Stannard and McIlwrath (1982) using the MERLIN array at 75 cm show that most of the flux in this feature comes from a compact component 3″ east of the nucleus, but there is also a much fainter "curved jet" feature emanating from the nucleus. If the halo were fainter, this source would have been included in Table 2 and classified as CBH. The source has also been observed briefly by Weiler and Johnston at 6 cm. From all the available radio data, there is no evidence that the nuclear radio component varies at either 6 or 20 cm. The polarization map shown in Figure 2*d* is interesting. The diffuse radio structure is rather strongly polarized ($\sim 10\%$), and the "jet" even more so (16.4%). The Galactic coordinates are $l = 2°$, $b = 70°$. Nearby radio sources exhibit rotation measures mainly in the range ± 5 radians m^{-2} (Simard-Normandin, Kronberg, and Button 1981). This, together with the high degree of polarization (indicating little *internal* Faraday rotation), suggests that the polarization position angles may be (very roughly) indicative of the magnetic field structure. If this is the case, then the magnetic field is mainly circumferential in the diffuse radio lobes (cf. Laing 1981) and is nearly parallel to the direction of elongation in the "jet" feature (cf. Bridle 1982). Obviously, shorter wavelength observations are necessary to confirm this.

l) 1727+502 = I Zw 186 = OT 546

This is a galaxy with a redshift of 0.055 (Miller, French, and Hawley 1978). The optical nucleus is variable and moderately polarized (Kinman 1976). It is not a radio variable (Bregman *et al.* 1982). Because of bad weather, we have only a single "snapshot" of this source. The radio structure consists of an unresolved core and faint diffuse halo. Weiler and Johnston (1980) detected the core at 6 cm but not any extended structure. The core has a flat spectrum ($\alpha \sim -0.05$). If the halo has a steep spectrum, Weiler and Johnston would have had great difficulty seeing it. We can set an upper limit of 0.01 Jy on any small-scale structure in the vicinity of the core.

m) 2155−152 = OX−192

This is a lineless BL Lac object. We have observed its optical polarization to be $P = 23\% \pm 1\%$, $\theta = 36° \pm 1°$ in 1980 August. Historical records show it to vary between 12th and 19th magnitude (Craine *et al.* 1976) with frequent outbursts with amplitudes of ~ 3 mag. It is also a well-known radio variable (Altschuler and Wardle 1976; Andrew *et al.* 1978). Weiler and Johnston (1980) detect extended structure of size $\sim 6''$ containing 0.16 Jy at 6 cm. The extended structure therefore has a spectral index of $\alpha = -0.7$. Perley (1982) finds the source to be triple, extended 5″.5 in position angle 0°. This agrees with our observations.

n) 2155−304

This is a BL Lac object. From faint emission lines, a tentative redshift of 0.17 has been suggested (Charles, Thorstensen, and Bowyer 1979). The optical nucleus is variable and moderately strongly polarized (Giffiths *et al.* 1979). Ulvestad, Johnston, and Weiler (1983) have also observed this source using the VLA at 20 cm. They find a total flux density of 0.33 Jy, of which 0.23 Jy is in a compact component. These agree with our results in Table 2. At 6 cm they find corresponding values of 0.32 Jy and 0.28 Jy. The core has a spectral index of $\alpha = +0.14$, and the extended structure has a spectral index of $\alpha \sim -0.7$. We present two maps of this source in Figures 1*g* and 1*h*. Figure 1*g* is at full resolution and shows the small-scale extended structure noted in Table 2. In Figure 1*h* the data have been tapered in the *u*-*v* plane with a Gaussian of width 30000λ (FWHM). The map shows a halo of diffuse emission extending mainly to the northwest and northeast. Ulvestad *et al.* show a map made with a $\sim 5000\lambda$ taper, which shows that the halo extends at least 1′ in the northwest and northeast directions. Such structure would be present on our low-resolution map at the level of ~ 0.3 mJy per beam. This is below our first contour, though we note the presence of several patches of emission at the level of ~ 1 mJy per beam. Clearly, we have missed the most diffuse part of the halo, and its overall size is greater than given in Table 2. However, 60% of its flux comes from a region $\sim 25''$ in extent.

o) 2254+074 = CTD 135 = OY 091

This is a lineless BL Lac object which is optically variable (Usher 1975) and exhibits strong and variable polarization (Kinman 1976). Wardle (1978) found the radio source to be variable at 3.7 and 11.1 cm. It has been observed several times with the VLA (Weiler and Johnston 1980; Ulvestad *et al.* 1981; Perley 1982), with no indication of extended structure. The strongest limits are from Perley, who sets limits at 20 and 6 cm of less than 0.7% and less than 0.6%, respectively, on the peak brightness of any extended structure.

We concur. Perley measured a flux density at 20 cm of only 0.35 Jy. It is clear that the source is quite variable at this wavelength also (see also Kühr *et al.* 1981).

p) 2345 − 167 = OZ − 176

This is a quasar with strong emission lines and a redshift of 0.60 (Hewitt and Burbidge 1980). It is optically variable (Pollock *et al.* 1979) with strong and variable polarization (Moore and Stockman 1981) and is also a radio variable (Altschuler and Wardle 1976; Andrew *et al.* 1978). The radio source is clearly dominated by a compact component, but there is no agreement as to the nature of any extended structure. Ulvested *et al.* (1981) classify the source as unresolved with no extended structure containing more than 10% of the total flux. They add in a footnote that they have subsequently found a halo which is resolved at 3 km antenna separation. They do not state the wavelength or give a flux density for the halo. Perley (1982), at 6 cm, found a 9 mJy component at a distance of 1″.8 from the core in position angle 355°. This is not the component we have found, which is at a distance of 4″ in position angle 230°. With our resolution, Perley's component would be difficult for us to see. It is possible we have underestimated the size of our component, and that it was resolved in Perley's observation. Perley's data at 20 cm do not shed any light on this problem. He lists a total flux density in parentheses and gives no information concerning extended structure. We are inclined to believe that the component we have found is real because it is visible on maps made both before and after the self-calibration procedure, but it is faint and further observations made with very high dynamic range are clearly desirable.

V. THE RELATIONSHIP BETWEEN OPTICAL POLARIZATION AND RADIO STRUCTURE

One of the original motivations for the radio observations was the idea that highly polarized quasars and BL Lac objects whose optical polarization exhibits a preferred position angle might be more likely to show extended radio structure. In this section, we consider this question. In addition, we examine whether there is a systematic correlation between the position angle of small-angle radio structure and the characteristic optical polarization position angle.

We have compiled relevant information in Table 4 to address these two questions. The sample consists of all BL Lac objects and highly polarized quasars which have been mapped by us or Ulvestad, Johnston, and Weiler (1983) and which have been well-monitored polarimetrically. Columns (1) and (2) of Table 4 list the source name and radio morphology as described in § III. The two sources in Table 4 dominated by two-sided extended structure, 0752 + 258 and 1400 + 162, have been classified as D1 sources. The objects are ordered in terms of a morphological sequence which characterizes the ratio of extended structure to core emission and the two-sidedness of the extended emission. The position angle of extended radio emission is given in column (3) for all sources with detected small-scale structure. Column (4) gives a measure of the relative prominence of the radio core at 20 cm, defined by the ratio $f_{20} \equiv S_{\text{central}}/S_{\text{extended}}$ (measured at 20.5 cm). We have applied a small "*K*-correction' by dividing the observed ratio by $(1 + z)^{0.75}$. This assumes that the radio core has a flat spectrum, and that the extended structure has a spectral index of −0.75. Where the redshift is unknown, we have assumed a value of $z = 0.4$. The source 2223 − 052 was not observed by Ulvestad *et al.* at 20.5 cm. At 2 cm they found the core was a small double source with a separation of 0″.15. We have deduced a value of f_{20} for this source by estimating what they would have observed at 20.5 cm with the VLA, given the information in their paper.

The characteristics of the position angle of optical polarization are described in columns (5)–(8). The mean position angle of the electric vector and its rms scatter are listed in columns (5) and (6). These are calculated from monthly averages of all published data (see Angel and Stockman 1980 for references) and our own unpublished data. A monthly average is first done to avoid weighting the results heavily by occasional epochs of intense monitoring; stability over time scales of months to years is required to demonstrate

TABLE 4

COMPARISON OF RADIO STRUCTURE AND OPTICAL POLARIZATION

	Radio Properties			Optical Properties				
Source (1)	Morph. (2)	Orient. (°) (3)	$\log f_{20}$ (4)	$\langle\theta\rangle$ (°) (5)	rms (°) (6)	N_M (7)	Class (8)	Δ (°) (9)
0752 + 258	D1	135	−1.71	146	3	8	P	11
1400 + 162	D1	90	−0.67	88	7	8	P	2
0219 + 428	CBH	161	0.05	24	9	6	P	43
0818 − 128	CBH	73	−0.17	87	21	9	P	14
1215 + 303	CBH	154	0.08	157	13	18	P	3
2155 − 304	CBH	90	0.21	159	9	4	P?	69?
1308 + 326	D2	0	1.14	...	38	9	R	...
2223 − 052	D2	90	2.04	...	61	12	R	...
1101 + 384	CH	...	0.39	170	18	14	P	...
1514 − 241	CH	...	1.24	175	32	10	R?	...
1652 + 398	CH	...	1.12	141	7	12	P	...
0235 + 164	C	...	> 2.11	...	90	7	R	...
0422 + 004	C	...	> 1.18	174	16	10	P	...
0735 + 178	C	...	> 2.20	5	23	20	P	...
2200 + 420	C	...	> 2.51	...	50	21	R	...

a preferred angle. The number of (lunar) months ($N_{\rm M}$) in which observations have been made is given in column (7). To be included in this sample of well-monitored objects, we require that data be available from at least 4 months over at least two observing seasons; most of the objects in Table 4 well exceed these minimum requirements. In column (8) each object is classified as having either a preferred (P) or random (R) position angle of polarization. This classification is based on the rms scatter of the observations, the total range of position angles exhibited, and the statistical probability of randomness. Details of this analysis and complete data for all BL Lac objects will be presented by Moore (1983). For all sources with both small-scale extended radio structure and a preferred position angle of polarization, the (unsigned) difference between these angles is listed in the final column.

Of the 15 sources in Table 4, four have random position angles of polarization, nine have preferred angles, and two have uncertain classifications. All of the random-angle objects are strongly core dominated, and none have two-sided structure. Also, all of the D1 and CBH sources have preferred angles of optical polarization. These tendencies are in the sense expected in the relativistic jet model, but the result is statistically weak because there are some sources with a preferred angle for optical polarization which have no detected extended radio structure.

We obtain a much stronger result if we compare the degree of enhancement of the radio core, measured by $\log f_{20}$, and the rms scatter of the position angle of optical polarization. A Spearman rank correlation test (e.g., Gibbons 1976) shows that these quantities are correlated at the 3.0 σ level of significance. This is exactly what is expected in the relativistic jet model, as discussed in § I.

Finally, we compare position angles of optical polarization and small-scale radio structure. There are five sources in Table 4 which have both extended structure and a preferred angle of polarization. In four of these, the position angles are aligned within 15°. If these angles were unrelated, the binomial probability of this occurring by chance is 0.4%. If we include 2155−304 (which has an uncertain classification), the probability that four of six would be aligned by chance is 1%.

The sample is small, and additional observations are clearly necessary to test this alignment among all preferred-angle BL Lac objects. However, the excellent agreement of angles among several objects in our sample provides strong evidence that the optical polarization is related to the radio structure in at least some highly polarized objects. Assuming that the optical emission is synchrotron radiation, the alignment of these angles implies that the magnetic field in the optical-emitting region is perpendicular to the direction of extended radio structure.

VI. ARE BL LAC OBJECTS "NORMAL DOUBLES" SEEN END ON?

So far we have discussed the extended radio structures we have found from a purely morphological point of view. In this section we consider the physical interpretation of the structures we have found, though in view of the small number of objects and the lack of any sort of complete sample, the discussion will be preliminary and mainly qualitative.

It is clear that many BL Lac objects do contain extended radio structure in addition to the compact radio source. Earlier surveys with an interferometer by Wardle (1978) and by Weiler and Johnston (1980) showed that about 50% of all known BL Lac objects contain some sort of extended structure. The detailed aperture-synthesis observations of Ulvestad, Johnston, and Weiler (1983) and those reported in this paper amply confirm this conclusion.

One possible interpretation of this extended structure follows naturally from the Scheuer-Readhead (1979) picture of compact radio sources, outlined in the Introduction. That is, we are looking at "normal" double radio sources, such as comprise the great majority of 3CR sources, nearly end-on (along their major axis), and the relative intensity of the central component is greatly enhanced by the Doppler effect. This has been discussed briefly by Perley, Fomalont, and Johnston (1980). Here we extend their discussion in light of our present results.

The first task is to characterize more precisely what is meant by a normal double source. We start from the complete sample of 199 extragalactic 3CR sources listed by Jenkins, Pooley, and Riley (1977), all of which have been observed with the Cambridge 5 km telescope with a resolution of a few arc seconds. Although many BL Lac objects show similar behavior to the OVV quasars (see Angel and Stockman 1980), whenever the underlying optical objects are studied in detail, both spectroscopy and surface photometry suggest they are elliptical galaxies (Miller and French 1978; Weistrop 1982; Miller 1981). We shall, therefore, restrict ourselves to the 59 radio sources in the Cambridge list that are identified with galaxies of known redshift. These 59 sources exhibit a wide variety of radio morphologies but have been divided into two broad categories by Fanaroff and Riley (1974). They measured the ratio of the distance between the regions of highest brightness on opposite sides of the galaxy to the total extent of the source measured from the lowest contour. (Any compact component coincident with the galaxy was not taken into account.) Those sources for which this ratio is less than 0.5 (emission concentrated near the center) were placed in class I; those for which the ratio is greater than 0.5 (emission concentrated near the outer edges) were placed in class II. We shall refer to the classes as FR I and FR II, respectively. Although this is an observational classification and depends to some extent on instrumental resolution and surface brightness sensitivity, the two classes are remarkably distinct. FR II sources are the "classical doubles" with "hotspots" close to the outer edges of any diffuse emission. FR I sources are of several types: "relaxed" doubles without hotspots (e.g., 3CR 28), head-tail sources (e.g., 3CR 83.1B), wide-angle tail sources (e.g., 3CR 465), and sources with prominent jets (e.g., 3CR 449). (The last three morphological types might be considered a single category [Owen and Rudnick 1976].) There is also a sharp division by intrinsic luminosity. Sources whose luminosity at 178 MHz is less than 2×10^{25} W Hz^{-1} sr^{-1} are almost exclusively in class I. Sources more luminous than this are almost exclusively in class II.

Of the 59 radio galaxies under consideration, 35 are in class II, and 17 are in class I. (We have used Fanaroff and Riley's assignments whenever possible.) Seven sources are completely dominated by an unresolved component.

Since any extended structure associated with these sources is not bright enough by itself to warrant inclusion in the 3CR catalog, we do not consider them further.

First, we shall compare the intrinsic luminosity of the extended structure surrounding BL Lac objects with that of the remaining 52 3CR radio galaxies. We include all the BL Lac objects with known redshifts which have been observed by us or by Ulvestad, Johnston, and Weiler (1983). Where only absorption redshifts are available, we take the highest redshift as being that of the radio source. Luminosities are computed at 6 cm emitted wavelength, assuming $H_0 = 50$ km s^{-1} Mpc^{-1} and $q_0 = 0$. The spectral index of the extended emission associated with the BL Lac objects is often not well known; where necessary, we have used $\alpha = -0.75$. The results for the BL Lac objects are listed in Table 5, and the comparison with 3CR radio galaxies is shown in Figure 3. (Although we have also observed a few highly polarized quasars, we do not consider them in this section, since it is not proper to compare them with 3CR galaxies.)

The division by luminosity between FR I and FR II is less marked at 6 cm than at long wavelengths because of the spread in spectral indices of the sources. The intrinsic luminosities of the extended radio structures surrounding the BL Lac objects (including the three sources that are not dominated by a compact radio source) range from low to average compared with the 3CR radio galaxies. Only in the case of the BL Lac object 0531−365 is the extended structure sufficiently bright to be included by itself in the 3CR catalog. But if the results of Fanaroff and Riley extend to lower flux density (i.e., they do not depend explicity on redshift), then Figure 3 suggests that BL Lac objects may be more closely related to FR I sources than to FR II sources. There is considerable overlap in the distributions, and BL Lac objects could of course be a mixture of the two classes. However, at least seven of the 14 BL Lac objects have extended radio structure that is less luminous than *any*

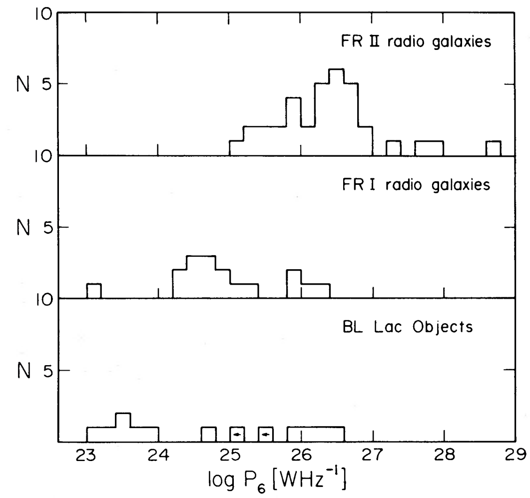

FIG. 3.—Comparison of the intrinsic luminosity at 6 cm of the extended radio structures associated with BL Lac objects and 3CR radio galaxies. The 3CR radio galaxies are divided into two categories based on their radio morphology (see text).

FR II radio galaxy in the 3CR sample. Since our sample of BL Lac objects is strongly biased in favor of sources that were known to have detectable extended radio structure, we consider this to be a strong result.

TABLE 5

INTRINSIC PROPERTIES OF BL LAC OBJECTS

Source	Redshift	log $P_6^{\rm ext}$ (W Hz^{-1})	$d^{\rm ext}$ (kpc)	log f_6
0219+428	0.444	26.58	757	0.09
0235+164	0.852	<25.44	...	>2.20
0521−365	0.061	26.14	65	−0.62
0735+178	0.424	<25.06	...	>2.23
0752+258	0.446	26.28	144	<−1.32
1101+384	0.031	23.55	172	1.33
1133+704	0.044	23.90	>60	0.14
1400+162	0.244	25.90	180	−0.26
1514−241	0.049	23.79	27	1.70
1652+398	0.034	23.31	56	1.49
1727+502	0.055	23.43	>15	0.91
2155−304	0.17	24.77	823	0.77
2200+420	0.069	<23.18	...	>2.81
0048−097	...	...	...	1.27
0422+044	...	...	...	>1.57
0818−128	...	...	...	0.23
0829+046	...	...	...	0.83
1215+303	...	...	...	0.78
1538+149	...	...	...	1.25
2155−152	...	...	...	0.79
2254+074	...	...	...	>1.44

Second, we consider the distribution of relative intensities of the central compact radio sources and the degree of Doppler boosting required to account for the prominence of the compact components in BL Lac objects. The distributions of the ratio $f_6 \equiv S_{\rm central}/S_{\rm extended}$ (measured at 6 cm) are shown in Figure 4. Since redshifts are not required, we have included all 22 BL Lac objects mapped by Ulvestad, Johnston, and Weiler (1983) and ourselves. For many of the 3CR galaxies, a central radio component is not detected by the 5 km telescope, and we have taken the lowest contour level on the published maps as an upper limit. For a few sources of small angular size, the position of the galaxy lies too close to an extended radio lobe to make a very sensible determination of the flux density of the galaxy by itself. For completeness, we have taken an apparent flux density from the maps, but this is probably grossly in error, and these sources are shown hatched in Figure 4. For all sources we have used $S_{\rm extended} = S_{\rm total} - S_{\rm central}$, so that very diffuse emission regions that may not show up on the maps are included. For some of the BL Lac objects we had to use 21 cm observations, and we assume $\alpha_{\rm central} = 0.0$ and $\alpha_{\rm extended} = -0.75$. We also included a "$K$-correction" as described in § V.

The f-distributions for FR I and FR II sources are significantly different, with the FR I sources showing relatively more prominent central components. We are interested in the *median* values of f. For FR I sources, this is 0.08. For FR II sources, the median lies between 0.01 and 0.02, the uncertainty being due to the many upper limits. We adopt a value of 0.015. The f-distribution for the BL Lac objects is extremely broad, having a width of at least 10^4:1. The median value of f is close to 10.

From these numbers we can deduce the Lorentz factors of the nuclear jets in the Scheuer-Readhead picture. We will

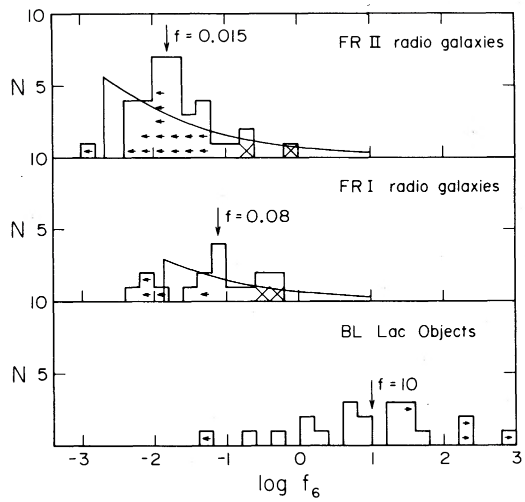

FIG. 4.—Comparison of the distributions of the ratio f_6($\equiv$ flux density of central component/flux density of extended structure) for BL Lac objects and 3CR radio galaxies. The arrows mark the median values of f_6 for each category.

assume (unrealistically) that the central components all have the same intrinsic value of f (different for FR I and FR II sources), and that the observed distribution corresponds to the distribution of Doppler enhancement factors due to differing orientations of the jets with respect to the line of sight. If the value of f observed when a jet is in the plane of the sky is f_{90}, then a jet pointing at an angle θ to the line of sight will have $f_\theta = f_{90}[1 - (v/c)\cos\theta]^{-(3+\alpha)}$, where v is the velocity of the jet, and c is the velocity of light (Ryle and Longair 1967). In certain circumstances an index of $-(2+\alpha)$ is appropriate (cf. Scheuer and Readhead 1979). We use $-(3+\alpha)$ because it leads to smaller Lorentz factors and strengthens the arguments that follow.

The quantities we wish to calculate are f_{90} and v/c. The 3CR radio galaxies are presumably oriented at random since the central components contribute negligible flux density at 178 MHz. The median value of θ is therefore 60°, and the median value of f corresponds to this angle. The BL Lac objects are, by hypothesis, all oriented at small values of θ. The maximum degree of Doppler enhancement occurs when $\theta = 0$, but such a special orientation is vanishingly rare. In practice, a typical group of prominent BL Lac objects will have values of θ clustered close to zero, and their nuclear fluxes will be boosted by somewhat less than the maximum factor. However, we wish to calculate a lower bound on v/c, so we shall take $\theta = 0$ for all the BL Lac objects. The median value of f then corresponds either to the median value of v/c, if there is a spread in v/c (as is likely), or to the median value of f_{90}, if there is a spread in that quantity (as is also likely). That is, we take the median value of f to correspond to a *typical* BL Lac object, oriented at $\theta = 0$.

From the above considerations we can write

$$f_{90}\left(1 - \frac{v}{c}\right)^{-(3+\alpha)} = 10\,,$$

$$f_{90}\left(1 - 0.5\,\frac{v}{c}\right)^{-(3-\alpha)} = \begin{cases}0.08 & \text{(for FR I sources)}\\ 0.015 & \text{(for FR II sources)}\end{cases}.$$

It follows immediately that if BL Lac objects are FR I sources seen end-on, then the nuclear radio sources must typically have $v/c > 0.89[\gamma \equiv (1 - v^2/c^2)^{-1/2} > 2.2]$. If BL Lac objects are FR II sources seen end-on, then the nuclear radio sources must typically have $v/c > 0.94(\gamma > 2.9)$. For reasons mentioned above, we consider these rather strong lower limits. Certainly, much larger values of v/c would be required to account for sources like BL Lac itself, for which $f \gtrsim 1000$. The values of f_{90} that follow from this argument are 0.014 for FR I sources and 0.002 for FR II sources.

We now ask if these values of v/c are compatible with other properties of 3CR radio galaxies. First, we calculate the expected distributions of f, given f_{90} and v/c (cf. Scheuer and Readhead 1979; Perley, Fomalont, and Johnston (1980). This is given by

$$dn = \left[\frac{v}{c}(3+\alpha)\right]^{-1}\left(\frac{f}{f_{90}}\right)^{-1-[1/(3+\alpha)]}\frac{df}{f_{90}}\,,$$

$$f_{90} \le f \le f_{90}\left(1 - \frac{v}{c}\right)^{-(3+\alpha)}.$$

In this simple picture, there are no further free parameters, and the distributions are shown in Figure 4. FR II sources do not fit the expected distribution very well. Nothing much can be said about the fit at low f because of the many upper limits, but there appears to be a lack of 3CR sources with large f. For FR II sources we expect 8.3 sources with $0.1 < f < 10$. We observe probably only two sources and certainly not more than four sources in this range. For larger values of v/c, the discrepancy becomes more troublesome. Note that sources with extended structure that falls into this range of f-values would be easily detected and resolved by the 5 km telescope. The "missing" sources cannot be the seven unresolved sources that we excluded from the 3CR sample. FR I sources may also show a deficit at large values of f, but the statistics are very poor. The point is simply that if the central components of 3CR radio galaxies are beamed sufficiently to resemble BL Lac objects when viewed end-on, then there should be an appreciable number of moderately high-f sources in an isotropic sample. These do not appear to be present.

The result of these arguments is that if we insist that BL Lac objects are "normal" radio galaxies seen end-on, then they are more likely to be FR I sources: the luminosities of the extended structures are more compatible, and we require lower Lorentz factors for the central component. However, from the distribution of f (the ratio of the central component flux density to the flux density of the extended structure), it is not clear that the central components of the *average* radio galaxy (FR I or FR II) have a large enough Lorentz factor to make them resemble the *average* BL Lac object, if seen end-on.

In order to quantify our arguments we have used an unrealistic model, in which all sources have the same values of v/c and f_{90}. In the real world we would expect there to be a spread in both quantities. BL Lac objects might then correspond to normal, but rarer, radio galaxies which fall on the high end of the v/c distribution. In this way we could also account for the very high-f sources like BL Lac itself. This idea seems reasonable for FR I sources but cannot work for FR II sources because the space density of high-luminosity radio galaxies is too low. The luminosity function of radio galaxies (at 400 MHz) has been constructed by Merkelijn (1971). The division between FR I and FR II radio sources occurs at about $P_{400} = 10^{25}$ W Hz^{-1} sr^{-1}. Scaling Merkelijn's results to a Hubble constant of 50 km s^{-1} Mpc^{-1}, the local space density of radio galaxies with $P_{400} \geq 10^{25}$ W Hz^{-1} sr^{-1} is about 140 Gpc^{-3}. Setti (1978) has estimated the space density of BL Lac objects as ~ 30 Gpc^{-3}. Schwartz and Ku (1983) have estimated the space density of X-ray emitting BL Lac objects ($L_x > 10^{44}$ ergs s^{-1}) as 130 Gpc^{-3}. Thus, there are not enough high-luminosity radio galaxies in the sky for BL Lac objects to be a rare subgroup of FR II sources, since there must be $\sim\gamma^2$ "normal-looking" radio galaxies for every core-dominated radio galaxy (Scheuer and Readhead 1979). These arguments are not relevant to FR I sources because the radio luminosity function is steep. From the data of Merkelijn and of Colla *et al.* (1975), we estimate the space density of radio galaxies with $10^{23} < P_{400} < 10^{25}$ W H$_\zeta^{-1}$ sr^{-1} to be 1–2 × 10^4 Gpc^{-3}: there is no shortage of them.

We must mention two possible difficulties with this interpretation. Madejski, Schuartz, and Ku (1982) have deduced Doppler beaming factors for 16 X-ray emitting BL Lac objects, based on a simple synchrotron self-Compton model. They find a wide range of Doppler factors with at least one-third being less than unity. They infer from this that the ejection directions are nearly isotropic. This would not be consistent with our interpretation of the core-dominated radio structures. Second, F. Owen (private communication) has surveyed the radio sources in a large number of Abell clusters (where only FR I sources are found) and has not found any BL Lac objects.

We have provided several independent pieces of evidence that BL Lac objects are *not* related to the high-luminosity, limb-brightened, classical double sources, such as Cygnus A. It appears possible (though we certainly have not proved it to be the case) that they may be low-luminosity FR I sources seen end-on. If this is so, the Lorentz factors required to account for the BL Lac objects in our sample are in the range $\gamma \sim 2$–4. This is higher than what appears to be the typical Lorentz factor in the central components of FR I sources from the 3CR sample. The difference could probably be ascribed to obvious selection effects.

We note that large-scale radio jets occur in at least 70% of low-luminosity radio galaxies but are less common among high-luminosity radio galaxies (Bridle 1982). We suspect that the small-scale extended structures we have found surrounding several BL Lac objects may in fact be large-scale jets seen end-on. The variety and complexity of these structures can be attributed to bends in the jets, seen greatly foreshortened. Further observations may lead to interesting constraints on the jet kinematics.

VII. SUMMARY

We have presented high dynamic range VLA maps of 16 BL Lac objects and highly polarized quasars. Extended radio structure with a variety of morphologies is common in our sample. Three of the sources (0521−365, 0752+258, and 1400+162) are dominated by extended structure with a fairly well-defined orientation (D1). The remaining sources are dominated by an unresolved component coincident with the optical nucleus. Six of these sources have barlike small-scale structure which surrounds the central core (CB or CBH), and two have one-sided extended emission (D2). No small-scale extended structure was detected for five sources (C or CH).

There is weak evidence for a connection between preferred position angles of optical polarization and radio morphology. Preferred-angle objects are more likely to exhibit two-sided (D1 or CBH) radio structure than random-angle objects. However, not all objects with preferred angles have extended structure. There is a much stronger correlation found between the prominence of the radio core and the rms scatter in the position angle of the optical polarization. These effects are precisely what is expected in the relativistic jet model.

Although the sample is small, there is remarkably good agreement between the position angle of the small-scale radio structure and the characteristic angle of optical polarization. Four of five (perhaps six) sources are aligned within 15°. This result is statistically significant and implies that, at least in some highly polarized objects, the magnetic field of the central optical-emitting region is related to the collimation direction of the radio jet.

A comparison of the luminosity of the extended radio emission of BL Lac objects to that of "normal" 3CR radio galaxies excludes the possibility that BL Lac objects are FR II sources seen end-on. The luminosity distribution of the extended emission is more comparable to that of FR I sources. Similarly, the distribution of the ratio of core to extended emission and the relative space densities are incompatible with BL Lac objects being relativistically enhanced end-on FR II sources, but are compatible with their being end-on FR I sources.

In general, our results can be successfully interpreted within the context of the relativistic jet model. This is not to say that we have proved this model to the exclusion of other models. A more detailed analysis requires that radio observations be made of a larger, more uniform sample. In addition, it is of particular interest to determine the optical polarimetric morphology of additional highly polarized objects and to test the alignment of optical polarization and radio structure for a larger sample of objects. Finally, the galaxies associated with FR I radio sources should be observed to find or set limits on unresolved optical nuclei that could be identified with "misdirected BL Lac objects." Under the very best seeing conditions, this can probably be accomplished with ground-based telescopes.

Since this paper was written, Browne (1983) has published a paper in which he reaches similar conclusions regarding the "parent population" of BL Lac objects.

REFERENCES

Altschuler, D. R. 1982, *A.J.*, **87**, 387.
Altschuler, D. R., and Wardle, J. F. C. 1976, *Mem. R.A.S.*, **82**, 1.
Andrew, B. H., Macleod, J. M., Harvey, G. A., and Medd, W. J. 1978, *A.J.*, **83**, 863.
Angel, J. R. P., *et al.* 1978, in *Pittsburgh Conference on BL Lac Objects*, ed. A. M. Wolfe (Pittsburgh: University of Pittsburgh Press), p. 117.
Angel, J. R. P., and Stockman, H. S. 1980, *Ann. Rev. Astr. Ap.*, **18**, 321.
Antonucci, R. R. J. 1982, *Nature*, **299**, 605.
Baars, J. W. M., Genzel, R., Pauliny-Toth I. I. K., and Witzel, A. 1977, *Astr. Ap.*, **61**, 99.
Baldwin, J. A., *et al.* 1977, *Ap. J.*, **215**, 408.
Blandford, R. D., and Königl, A. 1979, *Ap. J.*, **232**, 34.

Blandford, R. D., and Rees, M. J. 1978, in *Pittsburgh Conference on BL Lac Objects*, ed. A. M. Wolfe (Pittsburgh: University of Pittsburgh Press), p. 328.
Bregman, J. N., *et al.* 1982, *Ap. J.*, **253**, 19.
Bridle, A. H. 1982, in *IAU Symposium 97, Extragalactic Radio Sources*, ed. D. S. Heeschen and C. M. Wade (Dordrecht: Reidel), p. 121.
Browne, I. W. A. 1983, *M.N.R.A.S.*, **204**, 23P.
Charles, P., Thorstensen, J., and Bowyer, S. 1979, *Nature*, **281**, 285.
Cohen, M. H., and Unwin, S. C. 1982, in *IAU Symposium 97, Extragalactic Radio Sources*, ed. D. S. Heeschen and C. M. Wade (Dordrecht: Reidel), p. 345.
Colla, G., Fanti, C., Fanti, R., Gioia, I., Lari, C., Lequeux, J., Lucas, R., and Ulrich, M.-H. 1975, *Astr. Ap.*, **38**, 209.
Condon, J. J., Ledden, J. E., O'Dell, S. L., and Dennison, B. 1979, *A.J.*, **84**, 1.
Conway, R. G., and Stannard, D. 1972, *M.N.R.A.S.*, **160**, 31P.
Craine, E. R., Strittmatter, P. A., Tapia, S., Andrew, B. H., Harvey, G. A., Gearhart, M. R., and Kraus, J. D. 1976, *Ap. Letters*, **17**, 123.
Danziger, I. J., Fosbury, R. A. E., Goss, M. N., and Ekers, R. D. 1979, *M.N.R.A.S.*, **188**, 415.
Fanaroff, B. L., and Riley, J. M. 1974, *M.N.R.A.S.*, **167**, 31P.
Fanti, R., Ficarra, A., Mantovani, F., Padrielli, L., and Weiler, K. 1979, *Astr. Ap. Suppl.*, **36**, 359.
Gibbons, J. D. 1976, *Nonparametric Methods for Quantitative Analysis* (Holt, Reinhart and Winston).
Gopal-Krishna. 1977, *Nature*, **269**, 780.
Griffiths, R. E., Tapia, S., Briel, U., and Chaisson, L. 1979, *Ap. J.*, **234**, 810.
Hewitt, A., and Burbidge, G. R. 1980, *Ap. J. Suppl.*, **43**, 57.
Hintzen, P., and Owen, F. 1981, *A.J.*, **86**, 1577.
Hogböm, J. A. 1974, *Astr. Ap. Suppl.*, **15**, 417.
Jenkins, C. J., Pooley, G. G., and Riley, J. M. 1977, *Mem. R.A.S.*, **84**, 61.
Kesteven, M. J. L., Bridle, A. H., and Brandie, G. W. 1976, *A.J.*, **81**, 919.
Kinman, T. D. 1976, *Ap. J.*, **205**, 1.
Kühr, H., Witzel, A., Pauliny-Toth, I. I. K., and Nauber, U. 1981, *Astr. Ap. Suppl.*, **45**, 367.
Laing, R. A. 1981, *M.N.R.A.S.*, **195**, 261.
Landau, R., Epstein, E. E., and Rather, J. D. G. 1980, *A.J.*, **85**, 363.
Madejski, G. M., Schwartz, D. A., and Ku, W. H.-M. 1982, preprint.
Margon, B., Jones, T. W., and Wardle, J. F. C. 1978, *A.J.*, **83**, 1021.
Marscher, A. P. 1980, *Ap. J.*, **235**, 386.
Merkelijn, J. K. 1971, *Astr. Ap.*, **15**, 11.
Miley, G. K. 1971, *M.N.R.A.S.*, **152**, 477.
Miller, J. S. 1981, *Pub. A.S.P.*, **93**, 681.
Miller, J. S., and French, H. B. 1978, in *Pittsburgh Conference on BL Lac Objects*, ed. A. M. Wolfe (Pittsburgh: University of Pittsburgh Press), p. 228.
Miller, J. S., French, M. B., and Hawley, S. A. 1978, in *Pittsburgh Conference on BL Lac Objects*, ed. A. M. Wolfe (Pittsburgh: University of Pittsburgh Press), p. 176.
Moore, R. L. 1983, in preparation.
Moore, R. L., and Stockman, H. S. 1981, *Ap. J.*, **243**, 60.
Murdoch, H. S. 1976, *M.N.R.A.S.*, **177**, 441.
Owen, F. N., and Rudnick, L. 1976, *Ap. J.* (*Letters*), **205**, L1.
Perley, R. A. 1982, *A.J.*, **87**, 859.
Perley, R. A., Fomalont, E. B., and Johnston, K. J. 1980, *A.J.*, **85**, 649.
Pica, A. J., Pollock, J. T., Smith, A. G., Leacock, R. J., Edwards, P. L., and Scott, R. L. 1980, *A.J.*, **85**, 1442.
Pollock, J. T., Pica, A. J., Smith, A. G., Leacock, R. J., Edwards, P. L., and Scott, R. L. 1979, *A.J.*, **84**, 1658.
Ryle, M., and Longair, M. S. 1967, *M.N.R.A.S.*, **136**, 123.
Scheuer, P. A. G., and Readhead, A. C. S. 1979, *Nature*, **277**, 182.
Schwartz, D. A., and Ku, W. M.-H. 1983, *Ap. J.*, **266**, 459.
Setti, G. 1978, in *Pittsburgh Conference on BL Lac Objects*, ed. A. M. Wolfe (Pittsburgh: University of Pittsburgh Press), p. 385.
Simard-Normandin, M., Kronberg, P. P., and Button, S. 1981, *Ap. J. Suppl.*, **46**, 239.
Stannard, D., and McIlwrath, B. K. 1982, *Nature*, **298**, 140.
Stockman, H. S., Angel, J. R. P., and Miley, G. K. 1979, *Ap. J.* (*Letters*), **227**, L55.
Thompson, A. R., Clark, B. G., Wade, C. M., and Napier, P. J. 1980, *Ap. J.*, **44**, 151.
Ulvestad, J. S., Johnston, K. J., Perley, R. A., and Fomalont, E. B. 1981, *A.J.*, **86**, 1010.
Ulvestad, J. S., Johnston, K. J., and Weiler, K. W. 1983, *Ap. J.*, **266**, 18.
Usher, P. D. 1975, *Ap. J.* (*Letters*), **198**, L57.
Usher, P. D., Kolpanen, D. R., and Pollock, J. T. 1974, *Nature*, **252**, 365.
Wardle, J. F. C. 1978, in *Pittsburgh Conference on BL Lac Objects*, ed. A. M. Wolfe (Pittsburgh: University of Pittsburgh Press), p. 39.
Wardle, J. F. C., Bridle, A. H., and Kesteven, M. J. L. 1981, *A.J.*, **86**, 848.
Weiler, K. W., and Johnston, K. J. 1980, *M.N.R.A.S.*, **190**, 269.
Weistrop, D. 1982, in *IAU Symposium 97, Extragalactic Radio Sources*, ed. D. S. Heeschen, and C. M. Wade (Dordrecht: Reidel), p. 377.
Wills, B. J., and Wills, D. 1976, *Ap. J. Suppl.*, **31**, 143.

J. R. P. ANGEL: Steward Observatory, University of Arizona, Tucson, AZ 85721

RICHARD L. MOORE: Aerospace Corporation, P.O. Box 92957, Mail Code M4/934, Los Angeles, CA 90009

J. F. C. WARDLE: Physics Department, Brandeis University, Waltham, MA 02254